methods

Quantification of 3-ketodihydrosphingosine using HPLC-ESI-MS/MS to study SPT activity in yeast *Saccharomyces cerevisiae*

Jihui Ren,* Justin Snider,* Michael V. Airola,† Aaron Zhong,* Nadia A. Rana,* Lina M. Obeid,*,§, and Yusuf A. Hannun[1,†,*,§]**

Departments of Medicine* and Biochemistry and Cell Biology,† and Stony Brook Cancer Center,§ Stony Brook University, Stony Brook, NY 11794; and Northport Veterans Affairs Medical Center,** Northport, NY 11768

Abstract Serine palmitoyltransferase (SPT) catalyzes the rate-limiting step of condensation of L-serine and palmitoyl-CoA to form 3-ketodihydrosphingosine (3KDS). Here, we report a HPLC-ESI-MS/MS method to directly quantify 3KDS generated by SPT. With this technique, we were able to detect 3KDS at a level comparable to that of dihydrosphingosine in yeast *Saccharomyces cerevisiae*. An in vitro SPT assay measuring the incorporation of deuterated serine into deuterated 3KDS was developed. The results show that SPT kinetics in response to palmitoyl-CoA fit into an allosteric sigmoidal model, suggesting the existence of more than one palmitoyl-CoA binding site on yeast SPT and positive cooperativity between them. Myriocin inhibition of yeast SPT activity was also investigated and we report here, for the first time, an estimated myriocin K_i for yeast SPT of approximately 10 nM. Lastly, we investigated the fate of serine α-proton during SPT reaction. We provide additional evidence to support the proposed mechanism of SPT catalytic activity in regard to proton exchange between the intermediate NH_3^+ base formed on the active Lys residue with surrounding water. These findings establish the current method as a powerful tool with significant resolution and quantitative power to study SPT activity.—Ren, J., J. Snider, M. V. Airola, A. Zhong, N. A. Rana, L. M. Obeid, and Y. A. Hannun. **Quantification of 3-ketodihydrosphingosine using HPLC-ESI-MS/MS to study SPT activity in yeast *Saccharomyces cerevisiae*. *J. Lipid Res.* 2018.** 59: **162–170.**

Supplementary key words serine palmitoyltransferase • high-performance liquid chromatography-electrospray ionization-tandem mass spectrometry • sphingolipids

Sphingolipids are major membrane components that also play critical signaling roles in a plethora of essential cellular processes, such as cell proliferation, differentiation, apoptosis, and the inflammatory response (1). Dysregulation of their metabolism underlies various human diseases, such as type 2 diabetes, cancer, coronary artery diseases, inflammation, and neurological disorders, such as Alzheimer's and hereditary sensory and autonomic neuropathy type I (HSAN1) (2–4).

The sphingolipid biosynthetic pathway constitutes a complex network with many enzymes involved that generate and interconvert intermediate bioactive metabolites, such as ceramides and sphingosine-1-phosphate (5). Serine palmitoyltransferase (SPT) catalyzes the initial and rate-limiting reaction in the genesis of sphingolipids and it belongs to a subfamily of pyridoxal 5′-phosphate (PLP) enzymes known as α-oxoamine synthases. It catalyzes the condensation of L-serine with palmitoyl-CoA to form 3-ketodihydrosphingosine (3KDS) (6). The rate of this reaction directly controls the influx of amino acids and fatty acids into the sphingolipid pathway. Mutations in the human SPT subunit are associated with peripheral neuropathy HSAN1. As a critical enzyme and a potential drug target, the mechanism of SPT catalytic activity has been intensively studied.

SPT exists in all sphingolipid-producing organisms. The current proposed mechanism of SPT catalytic activity is mainly obtained through structural and functional studies using the prokaryotic system, bacterium *Sphingomonas paucimobilis* and *Sphingobacterium multivorum* (7–12). The mechanism of SPT catalytic activity and regulation is less

This work was supported by National Institutes of Health Grant R35 GM118128. Additional support was provided by American Heart Association Grant 17SDG33410860 (to M.V.A) and National Institutes of Health Grant F32 GM108384 (to N.A.R.). The content is solely the responsibility of the authors and does not necessarily represent the official views of the National Institutes of Health.

Manuscript received 14 June 2017 and in revised form 24 October 2017.

Published, JLR Papers in Press, November 1, 2017
DOI https://doi.org/10.1194/jlr.D078535

Abbreviations: DHS, dihydrosphingosine; IS, internal standard; 3KDS, 3-ketodihydrosphingosine; KDSR, 3KDS reductase; KIE, kinetic isotope effect; PLP, pyridoxal 5′-phosphate; SPT, serine palmitoyltransferase; SRM, selected reaction monitoring.

[1]To whom correspondence should be addressed.
e-mail: Yusuf.Hannun@stonybrookmedicine.edu

The online version of this article (available at http://www.jlr.org) contains a supplement.

known for its eukaryotic counterparts. Different from bacterial SPT, which is a soluble homodimer, eukaryotic SPTs exist as multi-subunit complexes, including the membrane-associated heterodimeric catalytic subunits and the regulatory subunits (13, 14). This was demonstrated by the purification of the SPOTS complex [SPT subunits (Lcb1/Lcb2), Orm1/2, Tsc3, and Sac1] in yeast and the identification of Tsc3 as positive and Orm1/2 as negative regulators of SPT activity (15–18). These regulatory mechanisms are conserved in the higher eukaryotic system with the identification of small subunits of mammalian SPT, ssSPTa/ssSPTb, as positive and mammalian ORMDL 1–3 as negative regulators of SPT (18, 19).

Accurate measurement of SPT activity is essential to study its mechanism of action and regulation. Multiple such assays have been developed, including using radiolabeled serine or palmitoyl-CoA as substrate to measure their incorporation into the organic phase consisting mainly of radiolabeled 3KDS, measurement of release of free CoA accompanied by SPT reaction, and HPLC to measure the fluorescent derivatives of dihydrosphingosine (DHS) (20–25). These established methods have been widely used and have contributed greatly in studying SPT activity in various organisms and their mechanism of action.

In this study, we developed a method using HPLC coupled with positive ESI followed by MS/MS to directly measure 3KDS generated by SPT. The current method represents a simplified procedure without additional derivation steps and it eliminates the usage of radioactive reagents and the associated cost and environmental issues. The method also showed high sensitivity and emerged as a reliable and quantitative tool to study SPT activity. With this tool, we obtained new insights into yeast SPT activity, including the possible existence of multiple palmitoyl-CoA binding sites in yeast SPT and the positive cooperativity between them. We report here an estimated myriocin K_i value for yeast SPT for the first time. Also the method enabled us to test the proposed catalytic mechanism of SPT and the results showed that the α-hydrogen of serine was completely replaced by protons from surrounding water during SPT reaction from yeast *Saccharomyces cerevisiae*.

MATERIALS AND METHODS

Materials

C17-SPH and DHS were purchased from Avanti Polar Lipids (Alabaster, AL). The 3KDS was from Matreya LLC (State College, PA). L-Ser (3,3-D2) and L-Ser (2,3,3,-D3) were obtained from Cambridge Isotope Laboratories Inc. (Tewksbury, MA). EDTA-free protease inhibitor cocktail was obtained from Roche. Pierce BCA protein assay kit was from Thermo Fisher Scientific. DAmpTSC10 yeast strain was purchased from GE Dharmacon. All other reagents were from Sigma-Aldrich (St. Louis, MO).

Lipid analysis

Yeast was cultured in synthetic medium with 2% glucose to logarithmic phase before adding 5% TCA and was kept on ice for 15 min. Cells were spun down at 4,000 *g* for 5 min and washed with water twice. C17-SPH [internal standard (IS)] (50 pmol) was added to the cell pellet before lipid extraction. Cells ($\sim$2–4 × 10^8) were resuspended in 1 ml extraction buffer containing 65% isopropanol, 13% diethyl ether, 26% pyridine, and 0.13% ammonium hydroxide and disrupted by 300 μl of glass beads with a bead-beater for 3 min. The suspension was then incubated at 65°C for 15 min before centrifugation at 4,000 *g* for 5 min to collect the supernatant. The pellet was extracted one more time by resuspending in 1 ml of extraction buffer. The supernatants from these two extractions were combined. Solvents were dried under nitrogen gas and resuspended in 200 μl mobile phase B solution (2% formic acid and 1 mM ammonium formate in methanol). An aliquot of 10 μl was subjected to lipid analysis.

Lipid analysis was performed using a Thermo Fisher LC/MS system, including an Accela autosampler, a Thermo pump, and a TSQ Quantum triple quadrupole mass spectrometer. Lipid samples were injected and eluted from Agilent Poroshell 120 EC-C18 [4.6 × 50 mm, 2.7 μm particle size column with 50–98% methanol gradient generated from mobile phase A (2% formic acid and 2 mM ammonium formate in water) and mobile phase B (2% formic acid and 1 mM ammonium formate in methanol)]. The mass spectrometer was operated in multiple reaction monitoring positive ionization mode, monitoring the following transitions: *m/z* 286.2 > 268.2 for C17-SPH; *m/z* 300.2 > 270.3 for 3KDS; *m/z* 302.3 > 284.3 for DHS; *m/z* 302.2 > 270.3 for 3KDS (+2); *m/z* 303.2 > 271.3 for 3KDS (+3); *m/z* 304.3 > 286.3 for DHS (+2), and *m/z* 305.3 > 287.3 for DHS (+3). Data were collected and processed using Xcalibur software. The transitions are also summarized in **Table 1**.

Quantification of sphingoid bases is based on the target analyte/IS peak-area ratio. The target analyte concentration is calculated based on the calibration curve generated by a series of peak area ratios between synthetic target analyte and IS plotted against the analyte concentration using a linear regression model. The 3KDS and DHS were quantitated using calibration curves for each synthetic compound, respectively. No synthetic standards are available for 3KDS (+2) and 3KDS (+3) and they were quantitated using 3KDS calibration curves.

Yeast microsome membrane preparation

Yeast microsome membrane fractions were prepared by the method adapted from Pinto, Wells, and Lester (26). Briefly, yeast cells cultured to logarithmic phase were collected by centrifugation and washed twice in 50 mM potassium phosphate buffer (pH 7.0). The pellet was resuspended in lysis buffer containing 50 mM

TABLE 1. MS/MS parameters used for the listed analytes

Analyte	Elemental Composition	Parental (M+H) (*m/z*)	Product (M+H) (*m/z*)	Collision Energy (eV)
3KDS	$C_{18}H_{37}NO_2$	300.2	270.3	19
DHS	$C_{18}H_{39}NO_2$	302.3	284.3	15
3KDS (+2)	$C_{18}H_{35}D_2NO_2$	302.2	270.3	19
DHS (+2)	$C_{18}H_{37}D_2NO_2$	304.3	286.3	15
3KDS (+3)	$C_{18}H_{34}D_3NO_2$	303.2	271.3	19
DHS (+3)	$C_{18}H_{36}D_3NO_2$	305.3	287.3	15
C17-SPH	$C_{17}H_{35}NO_2$	286.2	268.3	17

potassium phosphate (pH 7.0), 2.5 mM EDTA, 5 mM DTT, and 1× protease inhibitor cocktail and disrupted with 0.5 mm-diameter glass beads using Biospec Mini-Beadbeater-16 for six cycles of 1 min beating followed by 2 min cooling on ice. Unbroken cells and debris were removed by centrifugation at 4,000 *g* for 10 min. The supernatant was centrifuged at 100,000 *g* for 1 h at 4°C. The pellet was homogenized with the lysis buffer and centrifuged at 100,000 *g* for 1 h. The resulting pellet was resuspended in the lysis buffer. Protein concentration was determined by BCA assay.

In vitro SPT activity assay

A 200 μl reaction containing 0.1 M HEPES, 5 mM DTT, 50 μM pyridoxal phosphate, 0–400 μM palmitoyl-CoA, 0–15.2 mM L-Ser/or L-Ser (3,3-D2)/or L-Ser (2,3,3-D3), and 200 μg yeast microsome protein was incubated at 30°C for 5 min. The reaction was stopped by adding 2 ml 0.5 N NH_4OH. After adding 25 pmol C17-SPH (IS for MS), lipids were extracted by adding 2.5 ml chloroform methanol (2:1) and vortexed vigorously. After centrifugation at 4,000 *g* for 5 min, the upper aqueous phase was removed and the lower organic phase was washed twice with 5 ml water. The organic phase was dried under nitrogen gas and reconstituted in 100 μl mobile phase B. Ten microliters were subjected to HPLC-ESI-MS/MS analysis to measure the incorporation of L-Ser (3,3-D2) or L-Ser (2,3,3-D3) into 3KDS (+2) or 3KDS (+3). SPT velocity was measured by the amount of 3KDS products generated per minute per milligram of microsome proteins. The kinetics of SPT activity were measured by varying concentrations of palmitoyl-CoA and L-Ser (3,3-D2) or L-Ser (2,3,3-D3).

Measurement of incorporation of deuterated L-serine into deuterated 3KDS and DHS in yeast culture

Yeast were cultured to logarithmic phase at 30°C in synthetic medium supplemented with 2% glucose and amino acids required for the auxotrophic marker. Cells were collected by centrifugation and resuspended in fresh medium at a density of ~1 OD600 (2×10^7 cells/ml). Around 7.6 mM of deuterium-labeled serine were added to the culture. Approximately 2–4 × 10^8 cells were collected at each time point (0, 15, 30, 60, 90, and 120 min) and treated with 5% TCA followed by washing twice with water. The 3KDS and DHS generated from deuterated serine substrate were detected as early as 15 min.

RESULTS

Detection and separation of 3KDS and DHS using HPLC-ESI-MS/MS

Sensitive and specific detection of 3KDS is essential to measure SPT activity. DHS is the downstream product of 3KDS in the de novo sphingolipid synthesis pathway, formed by reduction of 3KDS through 3KDS reductase (KDSR) (27). The 3KDS and DHS have similar structures with a 2 Da difference in molecular mass caused by the replacement of the keto group with a hydroxyl group at the C3 position. Clear separation and detection of each analyte is essential for accurate quantitation of 3KDS free of DHS contamination. Synthetic 3KDS and DHS compounds were applied to Agilent Poroshell 120 HPLC column EC-18 and eluted with methanol gradient in the presence of ammonium formate over a 1 h time course. A specific signature fragmentation pattern for each compound, 3KDS with a parent *m/z* at 300.2 and a transition of *m/z* 300.3 > 270.3; DHS with a parent *m/z* at 302.3 and a transition at *m/z* 302.3 > 284.3, was used for their detection under positive ion mode ESI-MS/MS. The full product ion spectrum of both 3KDS and DHS is shown in supplemental Fig. S1. MS parameters used for these compounds are also summarized in Table 1. Under these conditions, 3KDS and DHS showed ~0.3 min difference in retention time and they showed similar intensity (**Fig. 1A**, B). Transition specificity was verified, as no signal in DHS transition was observed when injecting only 3KDS, and, reciprocally, no signal in 3KDS

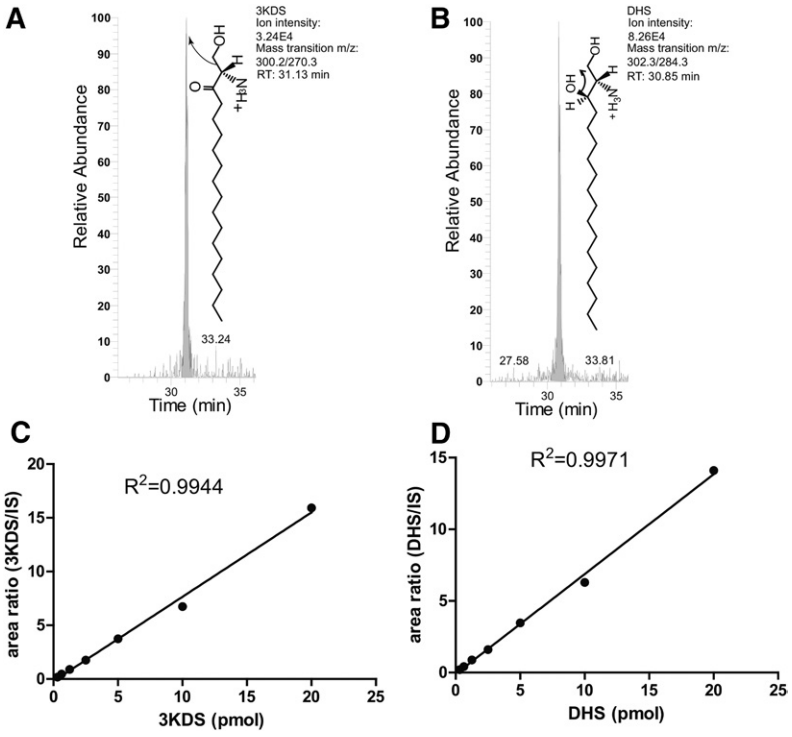

Fig. 1. Detection of 3KDS and DHS using HPLC-ESI-MS/MS. HPLC separation of 0.4 pmol 3KDS (A) and DHS (B) followed by positive mode ESI-MS/MS. Ion intensities, retention time (RT), and parent/product ion pairs are shown in the legends on the right of the SRM peaks. Also shown are the chemical structures of each compound and their fragmentation scheme. Calibration curves for 3KDS (C) and DHS (D). Calibration curves were established by detection of increasing amounts of 3KDS and DHS, respectively, using the transitions shown in A and B. The y-axis shows the peak area ratio of the analyte to C17-SPH (IS). Linear regression lines were generated by linear least-square fit with the regression coefficient displayed for each transition.

transition was observed when only DHS was injected. C17-SPH was used as IS for quantification of 3KDS and DHS. The ion product spectrum and selected reaction monitoring (SRM) peak of C17-SPH are shown in supplemental Fig. S2. Calibration lines were established with 0.3–20 pmol pure compounds in the presence of 2.5 pmol IS (Fig. 1C, D). The amount of compounds detected below the linear range was also plotted with the peak area ratio between analyte of interest and IS against their concentrations (supplemental Fig. S3). The observed detection limit for pure 3KDS and DHS compounds was around 10 fmol with a signal-to-noise ratio above 1,000.

After successfully separating and detecting 3KDS and DHS, we analyzed the whole cell lipid extract from the WT yeast, BY4741 (**Fig. 2A**). The 3KDS was detected at a level comparable to DHS, which is surprising, as it stands in contrast to the general concept that 3KDS is a very transient intermediate sphingoid base in the cell that normally falls below the detection limit. We next performed the same analysis using a yeast mutant in the same strain background, DAmPTSC10. TSC10 is an essential gene that encodes yeast KDSR, the enzyme that reduces 3KDS to form DHS, and the DAmPTSC10 strain is a mutant with decreased abundance of TSC10 transcript due to perturbation at the mRNA level (28). The results showed that attenuating TSC10 levels in the DAmPTSC10 strain resulted in marked accumulation of 3KDS and attenuation of DHS (Fig. 2A), thus further validating the specificity of the current 3KDS detection method. Whole cell lipids from several other commonly used *S. cerevisiae* WT strains were also measured, and comparable amounts of 3KDS and DHS were detected in all the strains tested, suggesting that the existence of a stable pool of 3KDS is a common phenomenon in yeast (Fig. 2B).

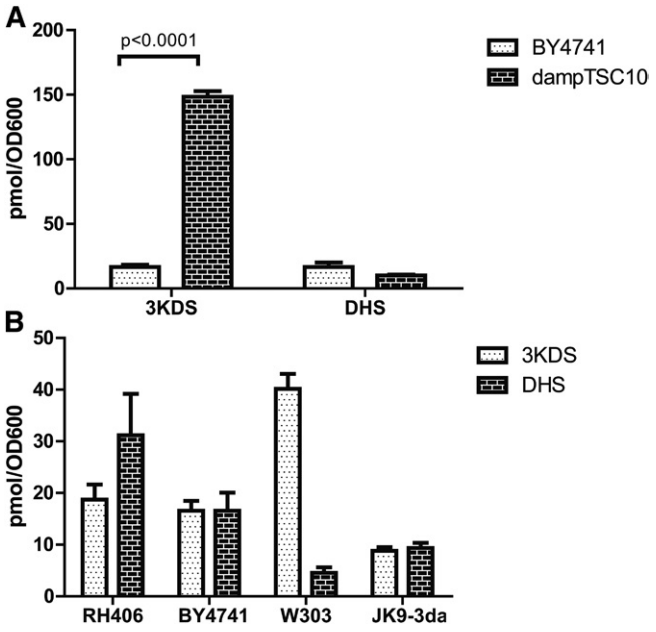

Fig. 2. Detection of 3KDS and DHS in yeast *S. cerevisiae*. A: Accumulation of 3KDS in the DAmPTSC10 strain. B: Existence of comparable amounts of 3KDS and DHS in the various commonly used yeast *S. cerevisiae* strains. Lipids were extracted from the indicated yeast strains cultured to logarithmic phase in YPD medium and subjected to HPLC-ESI-MS/MS to measure the levels of 3KDS and DHS.

Detection and separation of 3KDS (+2D) and DHS (+2D) generated from L-Ser (3,3-D2) using HPLC-ESI-MS/MS

Different from prokaryotic SPT, which can be recombinantly expressed and purified, most characterizations of eukaryotic SPT activity have been performed using crude cell lysates or microsome fractions, due to the difficulties in purifying soluble eukaryotic SPT. In this study, all the in vitro SPT assays were performed using yeast microsome fractions. In order to distinguish the endogenous 3KDS associated with the microsomal fraction from those acutely generated, we applied deuterated L-serine (3,3-D2) as the SPT substrate (**Fig. 3A**).

Figure 3B shows the result of an in vivo labeling experiment where deuterium-labeled 3KDS and DHS, 3KDS (+2D) and DHS (+2D), can be detected. They separate the same way on the column as their nondeuterated counterpart, and *m/z* 302.2 > 270.3 and *m/z* 304.3 > 286.3 are the new transitions used for 3KDS (+2D) and DHS (+2D), which generate the same fragmentation patterns. With this method, endogenous 3KDS and DHS could also be monitored at the same time using the aforementioned ESI-MS/MS collision parameters (data not shown).

SPT in vitro assay to study yeast SPT kinetics and its inhibition by myriocin

SPT activity from BY4741 microsomes was measured by conversion of L-Ser (3,3-D2) and palmitoyl-CoA into 3KDS (+2D) (**Fig. 4**). SPT kinetics in the presence of different concentrations of L-Ser (3,3-D2) were measured by plotting the initial velocity of the reaction against L-Ser (3,3-D2) concentration (Fig. 4A). Yeast microsomes (200 μg) and 200 μM of palmitoyl-CoA were used in all the assays. Under all the conditions tested, product formation was linear with time for the first 15 min and, therefore, a 5 min time point was used to stop the reaction in order to obtain the initial velocity. The data were fitted using the Michaelis-Menten equation yielding a K_m value for serine of 1.37 ± 0.4 mM and V_{max} of 387.6 ± 34.2 pmol/min/mg yeast microsome. This K_m for L-Ser (3,3-D2) is slightly lower than that reported for yeast SPT activity using the radiolabeled serine (26) and it is very similar to the reported K_m value for purified SPT from *S. paucimobilis*, where SPT kinetics were measured by monitoring the release of free CoA (10).

SPT kinetics, in the presence of different concentrations of palmitoyl-CoA, were measured by plotting the initial velocity of the reaction against various palmitoyl-CoA concentrations (Fig. 4B). Yeast microsomes (200 μg) and 15.2 mM of L-Ser (3,3-D2) were used in all of these assays. The data points were fitted better using the allosteric sigmoidal equation with an R-squared value of 0.96 (solid curve) than using the Michaelis-Menten equation, which yielded an R-squared value of 0.88 (dotted curve). The Hill coefficient was determined at 2.6 ± 1.2. This result suggests the existence of multiple binding sites for palmitoyl-CoA and positive cooperativity between the sites. The structure of SPT from

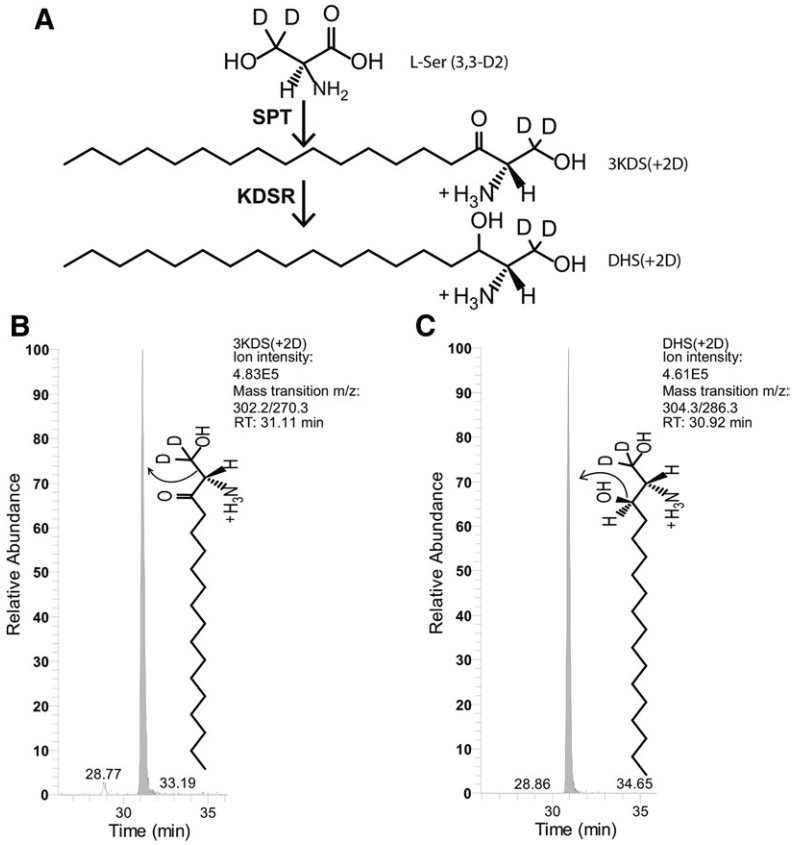

Fig. 3. Detection of 3KDS (+2D) and DHS (+2D) generated from L-Ser (3, 3-D2) using HPLC-ESI-MS/MS. A: Chemical structures of deuterated L-serine, 3KDS, and DHS [L-Ser (3,3-D2), 3KDS (+2D), and DHS (+2D)]. B: HPLC-ESI-MS/MS analysis of 3KDS (+2D) and DHS (+2D). Ion intensities, retention times (RT), and parent/product ion pairs are shown in the legends on the right of the SRM peaks. Also shown are the chemical structure of each compound and their fragmentation scheme. The 3KDS (+2D) (~19 pmol) and DHS (+2D) (~22 pmol) are generated from an in vivo labeling study where approximately 2×10^8 yeast cells were cultured in synthetic medium with 2% glucose to logarithmic phase before adding 7.6 mM L-Ser (3,3-D2) for 120 min. Total lipids were extracted and subjected to HPLC-ESI-MS/MS.

S. paucimobilis shows that it is a homodimer with two active substrate binding pockets (29). The catalytic subunit of yeast SPT is a heterodimer composed of Lcb1 and Lcb2 (17). Although no crystal structure is yet available for yeast SPT, it is reasonable to believe the existence of two substrate-binding pockets, just like its prokaryotic counterpart. Although the active Lys residue that is critical for its catalytic activity is missing from Lcb1, it is unlikely that this would negate binding of palmitoyl-CoA to this subunit.

Only marginal deuterium-labeled DHS signal [DHS (+2D)] was detected in this assay, and the signal did not increase with the increasing concentration of either palmitoyl-CoA or L-Ser (3,3-D2), suggesting insignificant KDSR activity under the current experimental conditions. With the current method, we were also able to detect endogenous 3KDS levels, and the results showed that they were maintained at a constant level during the course of the assay (data not shown), further supporting the conclusion that there is no significant KDSR activity in the system and that 3KDS is stable over the time of the assay. Thus, the 3KDS (+2D) generated from L-Ser (3,3-D2) represents SPT activity faithfully.

Myriocin is a potent SPT inhibitor that binds to SPT directly and competes with serine to form the external aldimine with PLP in the catalytic sites (30, 31). Using the SPT in vitro assay, we measured the inhibitory effects of myriocin

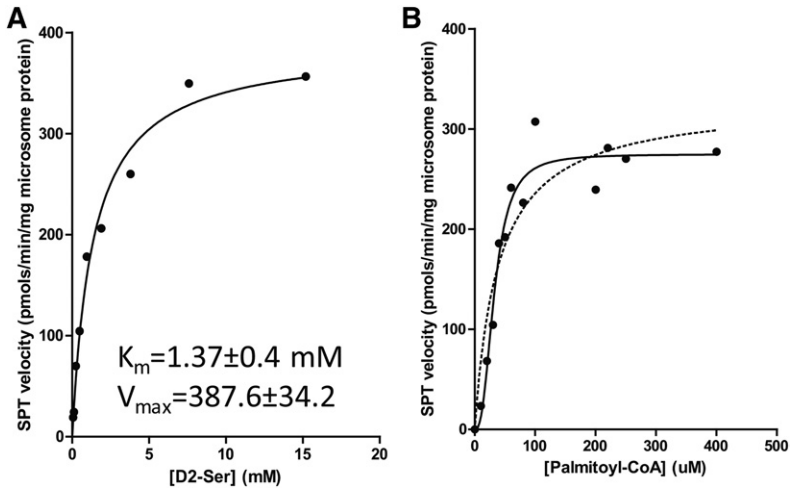

Fig. 4. In vitro assay to measure kinetics of SPT activity. SPT kinetics were measured by the amount of KDS (+2D) generated per milligram of microsomes per minute using L-Ser (3,3-D2) as SPT substrate. Microsomes were obtained from BY4741 cultured to logarithmic phase and used as SPT source for the reaction. A: SPT activity was measured in the presence of 200 μM palmitoyl-CoA with different concentrations of L-Ser (3,3-D2) ranging from 0 to 15.2 mM. Nonlinear regression curves were generated by least squares fit using Michaelis-Menten kinetics. Also shown are the K_m and V_{max}. B: SPT activity was measured in the presence of 15.2 mM L-Ser (3,3-D2) with different concentrations of palmitoyl-CoA ranging from 0 to 400 μM. The substrate velocity curve generated using an allosteric sigmoidal equation from GraphPad Prism 5 is shown as a solid curve. The substrate velocity curve generated using the Michaelis-Menten equation is shown as a dotted curve.

on yeast SPT by calculating the K_i (**Fig. 5**). SPT reaction rates in the presence of 0.95 mM L-Ser (3,3-D2) and various amounts of myriocin, ranging from 0 to 128 nM, were measured and plotted against myriocin concentrations. A K_i value of 10.3 ± 3.2 nM was calculated using the Morrison equation. In applying this equation, the K_m value for L-Ser (3,3-D2) was set to 1,370 μM, which was determined in an experiment without myriocin. The concentration of yeast SPT, which is required for the Morrison equation, was estimated at 0.0125 μM on the basis of 54,500 Lcb2 molecules per cell, reported by Ghaemmaghami et al. (32), and with the assumption that the microsome preparation efficiency was 50%. This estimated K_i value for yeast SPT is much lower than the reported myriocin K_i value (967 ± 98 nM) for the purified recombinant SPT from *S. paucimobilis* (31), suggesting a tighter binding of myriocin to yeast SPT.

Fate of α-hydrogen of serine during SPT reaction

The mechanism of SPT has been intensively studied and supplemental Fig. S4 shows the proposed PLP-dependent catalytic mechanism of SPT with L-Ser (2,3,3-D3) as the serine substrate (7–11, 33, 34). This model is composed of the following steps: Internal aldimine formed between PLP and the active lysine residue (presumably Lys366 of Lcb2 for yeast SPT) is displaced by the external aldimine formed between PLP and incoming serine substrate, in this case, L-Ser (2,3,3-D3). Binding of palmitoyl-CoA causes deprotonation of the external aldimine with the C2-deuterium extracted and transferred to Lys forming Lys-NH_2D^+, which could become Lys-NH_3^+ if exchange between deuterium with surrounding water occurs. Upon nucleophilic attack on the thioester, β-keto acid is formed accompanied by CoASH release. CO_2 is then released to form KDS product quinonoid, which is then reprotonated by abstraction of a proton from Lys-NH_3^+ or Lys-NH_2D^+. Lastly KDS is released, and the formation of internal aldimine between Lys and PLP is restored.

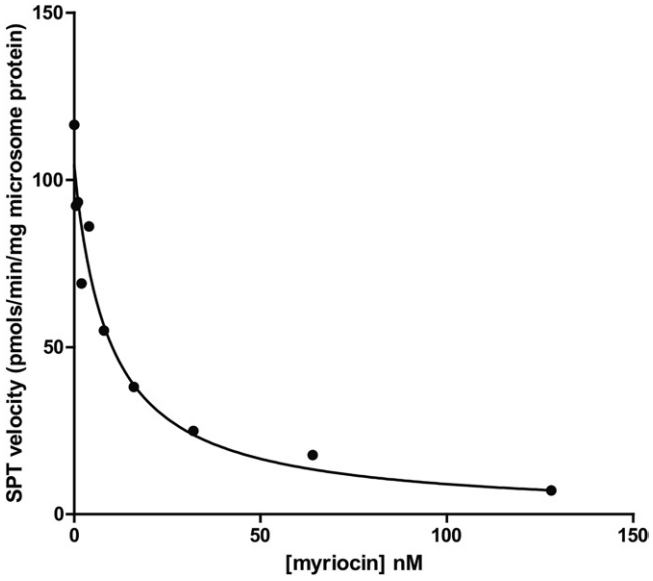

Fig. 5. Inhibition of yeast microsome SPT activity by myriocin. Two hundred micrograms of yeast microsomes (~0.0125 μM SPT) were incubated with 0.95 mM L-Ser (3,3-D2) in the presence of 0–128 nM myriocin for 5 min before stopping the reaction with NH_4OH followed by lipid extraction and HPLC-ESI-MS/MS to quantify the 3KDS (+2D) products. Enzyme activity, which was measured by SPT velocity, was plotted against myriocin concentration using the Morrison equation function from GraphPad Prism 5. The estimated K_i for myriocin is 10.3 ± 3.2 nM.

It has been proposed that the α-hydrogen of serine is readily replaced by a proton from medium during the SPT reaction. This is supported by in vitro SPT assays using deuterated serine at the C2 position [such as L-Ser (2,3,3-D3) in one study (35) or L-Ser (2,3,3-D3, 15N) in another (36)] as substrate and rat liver microsomes/whole cell of yeast (*Hansenula ciferri*)/ocean alga *Emiliania huxleyi* as SPT source. Instead of +3 or +4 products, labeled 3KDS product was only detected in the +2 or +3 form through GC-MS or LC-MS for each study, showing a complete loss of deuterium at the C2 position. In contrast, other studies have argued that the α-hydrogen of serine is retained during SPT reaction (37). That study measured the incorporation of tritium-labeled serine (at both the α and β position) into sphingolipids in rats and results from three out of seven experiments showed α-tritium was incorporated on the C2 position of sphingosine at the same ratio as β-tritium incorporation into the C1 position of sphingosine.

The currently developed assay, with an exquisite ability to distinguish the masses of the products, allowed for a direct test of the fate of serine α-hydrogen during SPT reaction. According to the proposed SPT catalytic mechanism, we would expect a complete replacement of a C2-deuterium with a hydrogen if there is a complete exchange between Lys-NH_2D^+ with bulk water. If no exchange between Lys-NH_2D^+ with bulk water occurs, we would expect to see a mixture of 3KDS products, some in which the C2-deuterium remains and some with it being replaced by one of the two hydrogens from the NH_2D^+. In order to test this with the newly developed HPLC-ESI-MS/MS method, we used L-Ser (2,3,3-D3) instead of L-Ser (3,3-D2) to determine the fate of the deuterium at the C2 position. In addition to detecting 3KDS (+2D) and DHS (+2D) using *m/z* 302.2/270.3 and *m/z* 304.3/286.3 collision pairs, we also detected significant amounts of 3KDS (+3) and DHS (+3) using *m/z* 303.2/271.3 and *m/z* 305.3/287.3 collision pairs in the in vivo labeling experiment (**Fig. 6**). We then confirmed this by the in vitro SPT assay (**Fig. 7**). The 3KDS (+3) and 3KDS (+2D) generated at each concentration of L-Ser (2,3,3-D3) were quantified and the ratio between them was calculated (**Table 2**). The ~18% ratio between 3KDS (+3) and 3KDS (+2D) is consistent with the probability of 3KDS (+2D) with one C13 atom per 3KDS (+2D) with primary C12 atoms. Because the natural abundance of C13 is 1.08 molecules per 100 atoms of C12 molecules, the probability for the positive ion fragment of 3KDS (+2D) containing one C13 atom is ~18% (~1.08% × 17). The results suggest that the signal detected by the 303.3/271.3 collision pair represents 3KDS (+2D) with one C13 atom instead of 3KDS (+3D). In order to further exclude the possibility that the signal detected with *m/z* 303.3/271.3 represents 3KDS (+3D), we collected MS/MS data using both

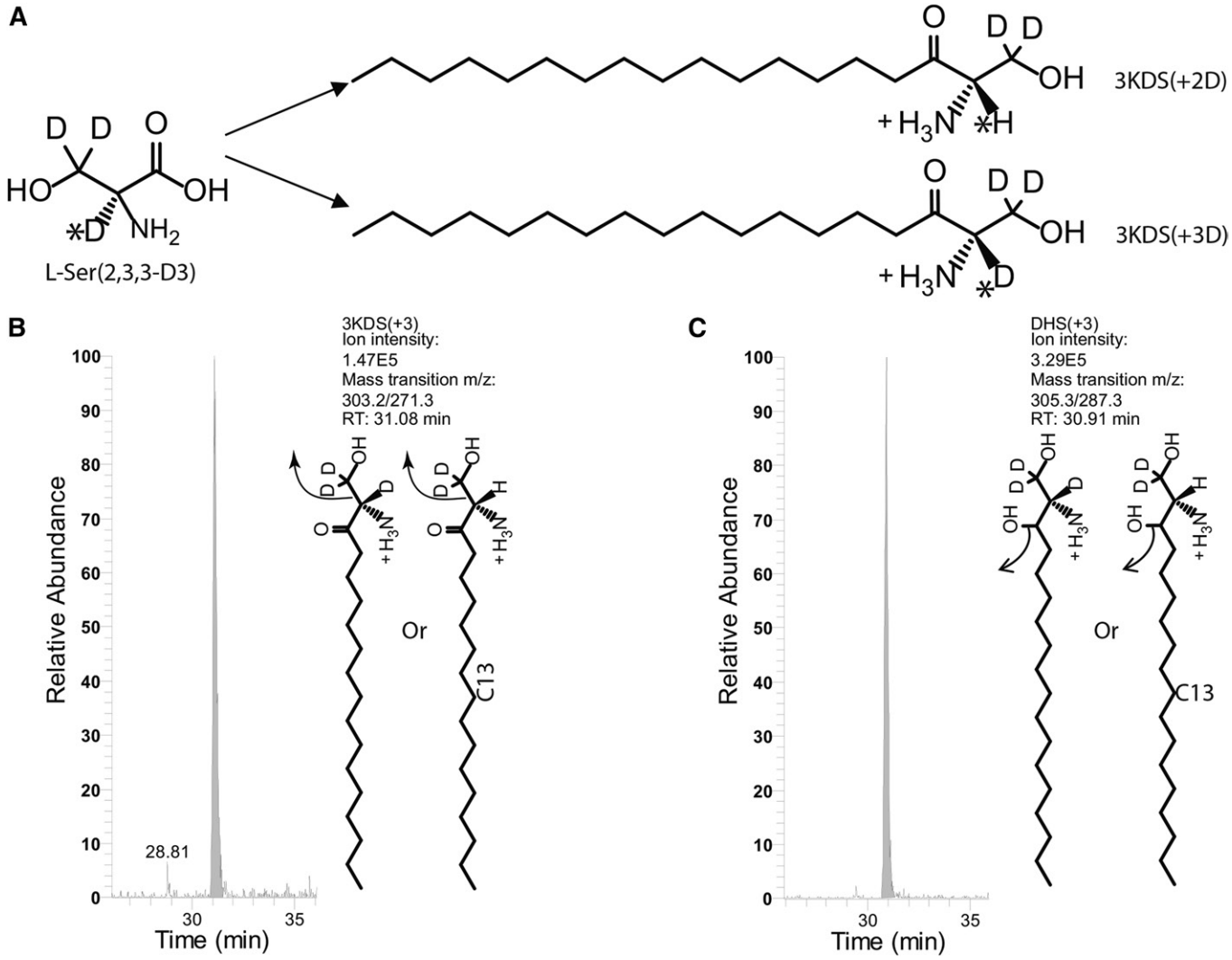

Fig. 6. Detection of 3KDS (+3) and DHS (+3) generated from L-Ser (2, 3, 3-D3) using HPLC-ESI-MS/MS. A: Chemical structures of L-Ser (2,3,3-D3) and possible deuterated 3KDS products, 3KDS (+2D) and 3KDS (+3D) depending on the fate of C2-deuterium. The C2 hydrogen/deuterium is marked by an asterisk. HPLC-ESI-MS/MS analysis of 3KDS (+3) (B) and DHS (+3) (C). Ion intensities, retention time (RT), and parent/product ion pairs are shown in the legends on the right of the SRM peak. Also shown are the chemical structure of each possible compound [3KDS (+3D) or 3KDS (+2D) with one C13 isotope, the C13 position is labeled randomly and it could be at any position from C2 to C18 for 3KDS and C1 to C18 for DHS] and their fragmentation scheme. The 3KDS (+3) (~5 pmol) and DHS (+3) (~15 pmol) are generated from an in vivo labeling study where approximately 2×10^8 yeast cells were cultured in synthetic medium with 2% glucose to logarithmic phase before adding 7.6 mM L-Ser (2,3,3-D3) for 120 min. Total lipids were extracted and subjected to HPLC-ESI-MS/MS.

m/z 303.3/271.3 and *m/z* 302.3/270.3 collision pairs for SPT in vitro assay with L-Ser (3.3-D2) as substrate. Signals were detected from both channels and their ratio is about 18% (data not shown). The results further confirm that the ~18% of 3KDS detected using the *m/z* 303.3/271.3 collision pair is the 3KDS (+2D) with one C13 carbon. This result supports a complete loss of C2-deuterium of serine during yeast SPT reaction.

L-serine with deuterium at the C2 position is a common reagent and constantly used as a substrate to study SPT activity. It is possible to cause a kinetic isotope effect (KIE) because this C2 deuterium is involved in the SPT catalytic reaction. In order to assess whether there was any KIE when using L-serine with C2-deuterium, an SPT kinetic assay was performed using L-Ser (2,3,3-D3) as substrate. The result showed that the K_m value is essentially the same by measuring SPT velocity using either the 3KDS (+2D) or the 3KDS (+2D) with one C13 product (Fig. 7). This K_m value, 1.3 ± 0.5, for L-Ser (2,3,3-D3) is also very similar to the K_m for L-Ser (3,3-D2). The reaction rate for 3KDS (+2D) production from L-Ser (3,3-D2) and that of 3KDS (+2D) production from L-Ser (2,3,3-D3) are also very similar (Figs. 4A, 7A). These results suggest that there is no KIE when using L-serine with C2-deuterium as substrate.

In summary, some previous studies claim a complete proton exchange during SPT reaction between the lysine base and the surrounding solvent (35, 36) and some argue against it (37). Our study supports a complete proton exchange during yeast SPT reaction by showing the generation of 3KDS (+2D) as the sole SPT product when using the L-Ser (2,3,3-D3) as substrate.

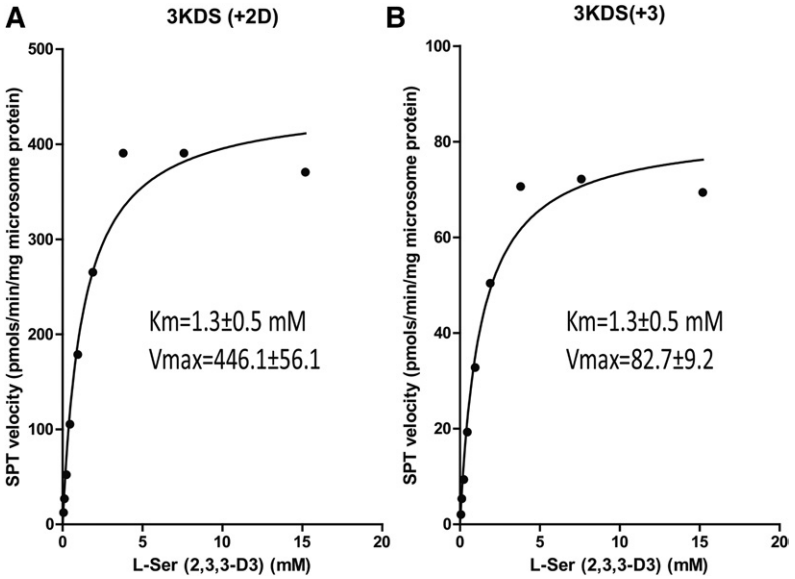

Fig. 7. Kinetics of SPT activity from WT yeast microsomes measured by production of 3KDS (+2) and 3KDS (+3) using L-Ser (2,3,3-D3) as substrate. Initial SPT velocity measured by production of 3KDS (+2D) (A) or 3KDS (+3) (B) per milligram of microsome per minute were plotted against different concentrations of L-Ser (2,3,3-D3) ranging from 0 to 15.2 mM using the Michaelis-Menten equation function from GarphPad Prism 5. Also shown are the K_m and V_{max}.

DISCUSSION

In this study, we developed a HPLC-ESI-MS/MS method to quantitatively measure 3KDS and DHS. The current approach shows great sensitivity and specificity in detecting cellular sphingoid bases. This is demonstrated by the detection of both cellular 3KDS and DHS in the absence of fumonisin B1, a ceramide synthase inhibitor that is commonly used to boost sphingoid base levels (22).

The robust quantification power of the current method is demonstrated by the detailed in vitro analysis of yeast SPT activity, which yielded several interesting observations, namely, the allosteric sigmoidal curve for palmitoyl-CoA binding, the higher myriocin binding affinity, and the complete exchange between serine α-hydrogen with the protons from surrounding bulk water during yeast SPT reaction. All of these provide new insights into the catalytic mechanism of eukaryotic SPT.

A point mutation in the bovine KDSR, FVT1, has been reported to associate with bovine spinal muscular atrophy (38). More recently, mutations in human KDSR have been reported to cause recessive progressive symmetric erythrokeratoderma (39) and keratinization disorders that associated with thrombocytopenia (40). We believe that the method developed here is a useful tool to further characterize these diseases by directly measuring the 3KDS level in patients. The 3KDS is considered an intermediate sphingolipid product with no cellular function of its own. Direct detection of a cellular pool of 3KDS will help to explore its possible role as a bioactive molecule.

The existence of diverse SPT substrates other than serine and palmitoyl-CoA as well as the enzyme's multiple regulatory subunits suggest that the enzyme complex is highly regulated in eukaryotic cells (26, 41–43). The approach we developed here has the potential to be modified so that it could be used in in vivo assays to help to elucidate the detailed regulatory mechanism of SPT.

TABLE 2. List of 3KDS products generated using L-Ser (2,3,3-D3)

L-Ser (2,3,3-D3) (mM)	*m/z* *302.2/270.2 (pmol)*	*m/z* *303.2/271.2 (pmol)*	*m/z* 303.2/271.2 (%)
0.06	12.5	2.1	16.8
0.12	27.1	5.4	19.9
0.24	52.3	9.4	17.9
0.48	105.4	19.3	18.3
0.96	178.7	32.8	18.3
1.9	265.3	50.4	18.9
3.8	390.6	70.6	18.1
7.6	390.7	72.2	18.5
15.2	370.6	69.4	18.7

Shown are 3KDS products detected using collision pairs, *m/z* 302.2/270.2 and *m/z* 303.2/271.2, and their percentage ratio at each L-Ser (2,3,3-D3) concentration used for the in vitro SPT assay in the presence of 200 μg microsomes from BY4741.

REFERENCES

1. Hannun, Y. A., and L. M. Obeid. 2008. Principles of bioactive lipid signalling: lessons from sphingolipids. *Nat. Rev. Mol. Cell Biol.* **9:** 139–150.
2. Bejaoui, K., Y. Uchida, S. Yasuda, M. Ho, M. Nishijima, R. H. Brown, Jr., W. M. Holleran, and K. Hanada. 2002. Hereditary sensory neuropathy type 1 mutations confer dominant negative effects on serine palmitoyltransferase, critical for sphingolipid synthesis. *J. Clin. Invest.* **110:** 1301–1308.
3. Kolter, T., and K. Sandhoff. 2006. Sphingolipid metabolism diseases. *Biochim. Biophys. Acta.* **1758:** 2057–2079.
4. Pralhada Rao, R., N. Vaidyanathan, M. Rengasamy, A. Mammen Oommen, N. Somaiya, and M. R. Jagannath. 2013. Sphingolipid metabolic pathway: an overview of major roles played in human diseases. *J. Lipids.* **2013:** 178910.
5. Ren, J., and Y. A. Hannun. 2017. Metabolism and roles of sphingolipids in yeast Saccharomyces cerevisiae. *In* Biogenesis of Fatty Acids, Lipids and Membranes. O. Geiger, editor. Springer International Publishing, Cham, Switzerland. 1–21.
6. Dickson, R. C., and R. L. Lester. 1999. Yeast sphingolipids. *Biochim. Biophys. Acta.* **1426:** 347–357.
7. Alexeev, D., R. L. Baxter, D. J. Campopiano, O. Kerbarh, L. Sawyer, N. Tomczyk, R. Watt, and S. P. Webster. 2006. Suicide inhibition of alpha-oxamine synthases: structures of the covalent adducts of 8-amino-7-oxononanoate synthase with trifluoroalanine. *Org. Biomol. Chem.* **4:** 1209–1212.
8. Hunter, G. A., and G. C. Ferreira. 1999. Lysine-313 of 5-aminolevulinate synthase acts as a general base during formation of the quinonoid reaction intermediates. *Biochemistry.* **38:** 3711–3718.

9. Kerbarh, O., D. J. Campopiano, and R. L. Baxter. 2006. Mechanism of alpha-oxoamine synthases: identification of the intermediate Claisen product in the 8-amino-7-oxononanoate synthase reaction. *Chem. Commun. (Camb.).* 60–62.
10. Raman, M. C., K. A. Johnson, B. A. Yard, J. Lowther, L. G. Carter, J. H. Naismith, and D. J. Campopiano. 2009. The external aldimine form of serine palmitoyltransferase: structural, kinetic, and spectroscopic analysis of the wild-type enzyme and HSAN1 mutant mimics. *J. Biol. Chem.* **284:** 17328–17339.
11. Webster, S. P., D. Alexeev, D. J. Campopiano, R. M. Watt, M. Alexeeva, L. Sawyer, and R. L. Baxter. 2000. Mechanism of 8-amino-7-oxononanoate synthase: spectroscopic, kinetic, and crystallographic studies. *Biochemistry.* **39:** 516–528.
12. Ikushiro, H., M. M. Islam, A. Okamoto, J. Hoseki, T. Murakawa, S. Fujii, I. Miyahara, and H. Hayashi. 2009. Structural insights into the enzymatic mechanism of serine palmitoyltransferase from Sphingobacterium multivorum. *J. Biochem.* **146:** 549–562.
13. Hanada, K., T. Hara, M. Nishijima, O. Kuge, R. C. Dickson, and M. M. Nagiec. 1997. A mammalian homolog of the yeast LCB1 encodes a component of serine palmitoyltransferase, the enzyme catalyzing the first step in sphingolipid synthesis. *J. Biol. Chem.* **272:** 32108–32114.
14. Nagiec, M. M., J. A. Baltisberger, G. B. Wells, R. L. Lester, and R. C. Dickson. 1994. The LCB2 gene of Saccharomyces and the related LCB1 gene encode subunits of serine palmitoyltransferase, the initial enzyme in sphingolipid synthesis. *Proc. Natl. Acad. Sci. USA.* **91:** 7899–7902.
15. Breslow, D. K., S. R. Collins, B. Bodenmiller, R. Aebersold, K. Simons, A. Shevchenko, C. S. Ejsing, and J. S. Weissman. 2010. Orm family proteins mediate sphingolipid homeostasis. *Nature.* **463:** 1048–1053.
16. Brice, S. E., C. W. Alford, and L. A. Cowart. 2009. Modulation of sphingolipid metabolism by the phosphatidylinositol-4-phosphate phosphatase Sac1p through regulation of phosphatidylinositol in Saccharomyces cerevisiae. *J. Biol. Chem.* **284:** 7588–7596.
17. Gable, K., H. Slife, D. Bacikova, E. Monaghan, and T. M. Dunn. 2000. Tsc3p is an 80-amino acid protein associated with serine palmitoyltransferase and required for optimal enzyme activity. *J. Biol. Chem.* **275:** 7597–7603.
18. Han, S., M. A. Lone, R. Schneiter, and A. Chang. 2010. Orm1 and Orm2 are conserved endoplasmic reticulum membrane proteins regulating lipid homeostasis and protein quality control. *Proc. Natl. Acad. Sci. USA.* **107:** 5851–5856.
19. Han, G., S. D. Gupta, K. Gable, S. Niranjanakumari, P. Moitra, F. Eichler, R. H. Brown, Jr., J. M. Harmon, and T. M. Dunn. 2009. Identification of small subunits of mammalian serine palmitoyltransferase that confer distinct acyl-CoA substrate specificities. *Proc. Natl. Acad. Sci. USA.* **106:** 8186–8191.
20. Merrill, A. H., Jr., and E. Wang. 1992. Enzymes of ceramide biosynthesis. *Methods Enzymol.* **209:** 427–437.
21. Ellman, G. L. 1959. Tissue sulfhydryl groups. *Arch. Biochem. Biophys.* **82:** 70–77.
22. Riley, R. T., W. P. Norred, E. Wang, and A. H. Merrill. 1999. Alteration in sphingolipid metabolism: bioassays for fumonisin- and ISP-I-like activity in tissues, cells and other matrices. *Nat. Toxins.* **7:** 407–414.
23. Rütti, M. F., S. Richard, A. Penno, A. von Eckardstein, and T. Hornemann. 2009. An improved method to determine serine palmitoyltransferase activity. *J. Lipid Res.* **50:** 1237–1244.
24. Dickson, R. C., R. L. Lester, and M. M. Nagiec. 2000. Serine palmitoyltransferase. *Methods Enzymol.* **311:** 3–9.
25. Williams, R. D., E. Wang, and A. H. Merrill, Jr. 1984. Enzymology of long-chain base synthesis by liver: characterization of serine palmitoyltransferase in rat liver microsomes. *Arch. Biochem. Biophys.* **228:** 282–291.
26. Pinto, W. J., G. W. Wells, and R. L. Lester. 1992. Characterization of enzymatic synthesis of sphingolipid long-chain bases in Saccharomyces cerevisiae: mutant strains exhibiting long-chain-base auxotrophy are deficient in serine palmitoyltransferase activity. *J. Bacteriol.* **174:** 2575–2581.
27. Beeler, T., D. Bacikova, K. Gable, L. Hopkins, C. Johnson, H. Slife, and T. Dunn. 1998. The Saccharomyces cerevisiae TSC10/YBR265w gene encoding 3-ketosphinganine reductase is identified in a screen for temperature-sensitive suppressors of the Ca2+-sensitive csg2Delta mutant. *J. Biol. Chem.* **273:** 30688–30694.
28. Breslow, D. K., D. M. Cameron, S. R. Collins, M. Schuldiner, J. Stewart-Ornstein, H. W. Newman, S. Braun, H. D. Madhani, N. J. Krogan, and J. S. Weissman. 2008. A comprehensive strategy enabling high-resolution functional analysis of the yeast genome. *Nat. Methods.* **5:** 711–718.
29. Beattie, A. E., S. D. Gupta, L. Frankova, A. Kazlauskaite, J. M. Harmon, T. M. Dunn, and D. J. Campopiano. 2013. The pyridoxal 5′-phosphate (PLP)-dependent enzyme serine palmitoyltransferase (SPT): effects of the small subunits and insights from bacterial mimics of human hLCB2a HSAN1 mutations. *BioMed Res. Int.* **2013:** 194371.
30. Chen, J. K., W. S. Lane, and S. L. Schreiber. 1999. The identification of myriocin-binding proteins. *Chem. Biol.* **6:** 221–235.
31. Wadsworth, J. M., D. J. Clarke, S. A. McMahon, J. P. Lowther, A. E. Beattie, P. R. Langridge-Smith, H. B. Broughton, T. M. Dunn, J. H. Naismith, and D. J. Campopiano. 2013. The chemical basis of serine palmitoyltransferase inhibition by myriocin. *J. Am. Chem. Soc.* **135:** 14276–14285.
32. Ghaemmaghami, S., W. K. Huh, K. Bower, R. W. Howson, A. Belle, N. Dephoure, E. K. O'Shea, and J. S. Weissman. 2003. Global analysis of protein expression in yeast. *Nature.* **425:** 737–741.
33. Zaman, Z., P. M. Jordan, and M. Akhtar. 1973. Mechanism and stereochemistry of the 5-aminolaevulinate synthetase reaction. *Biochem. J.* **135:** 257–263.
34. Yard, B. A., L. G. Carter, K. A. Johnson, I. M. Overton, M. Dorward, H. Liu, S. A. McMahon, M. Oke, D. Puech, G. J. Barton, et al. 2007. The structure of serine palmitoyltransferase; gateway to sphingolipid biosynthesis. *J. Mol. Biol.* **370:** 870–886.
35. Krisnangkura, K., and C. C. Sweeley. 1976. Studies on the mechanism of 3-ketosphinganine synthetase. *J. Biol. Chem.* **251:** 1597–1602.
36. Ziv, C., S. Malitsky, A. Othman, S. Ben-Dor, Y. Wei, S. Zheng, A. Aharoni, T. Hornemann, and A. Vardi. 2016. Viral serine palmitoyltransferase induces metabolic switch in sphingolipid biosynthesis and is required for infection of a marine alga. *Proc. Natl. Acad. Sci. USA.* **113:** E1907–E1916.
37. Weiss, B. 1963. The biosynthesis of sphingosine. I. A study of the reaction with tritium-labeled serine. *J. Biol. Chem.* **238:** 1953–1959.
38. Kihara, A., and Y. Igarashi. 2004. FVT-1 is a mammalian 3-ketodihydrosphingosine reductase with an active site that faces the cytosolic side of the endoplasmic reticulum membrane. *J. Biol. Chem.* **279:** 49243–49250.
39. Boyden, L. M., N. G. Vincent, J. Zhou, R. Hu, B. G. Craiglow, S. J. Bayliss, I. S. Rosman, A. W. Lucky, L. A. Diaz, L. A. Goldsmith, et al. 2017. Mutations in KDSR cause recessive progressive symmetric erythrokeratoderma. *Am. J. Hum. Genet.* **100:** 978–984.
40. Takeichi, T., A. Torrelo, J. Y. W. Lee, Y. Ohno, M. L. Lozano, A. Kihara, L. Liu, Y. Yasuda, J. Ishikawa, T. Murase, et al. 2017. Biallelic mutations in KDSR disrupt ceramide synthesis and result in a spectrum of keratinization disorders associated with thrombocytopenia. *J. Invest. Dermatol.* **137:** 2344–2353.
41. Dickson, R. C. 2008. Thematic review series: sphingolipids. New insights into sphingolipid metabolism and function in budding yeast. *J. Lipid Res.* **49:** 909–921.
42. Olson, D. K., F. Frohlich, R. V. Farese, Jr., and T. C. Walther. 2016. Taming the sphinx: mechanisms of cellular sphingolipid homeostasis. *Biochim. Biophys. Acta.* **1861:** 784–792.
43. Zitomer, N. C., T. Mitchell, K. A. Voss, G. S. Bondy, S. T. Pruett, E. C. Garnier-Amblard, L. S. Liebeskind, H. Park, E. Wang, M. C. Sullards, et al. 2009. Ceramide synthase inhibition by fumonisin B1 causes accumulation of 1-deoxysphinganine: a novel category of bioactive 1-deoxysphingoid bases and 1-deoxydihydroceramides biosynthesized by mammalian cell lines and animals. *J. Biol. Chem.* **284:** 4786–4795.